

INTERMEDIATE-MASS-FRAGMENT PRODUCTION IN THE REACTION OF 200 MeV ^3He WITH Ag^*

K. Kwiatkowski, J. Bashkin, H. Karwowski[†], M. Fatyga and V.E. Viola
 Indiana University Cyclotron Facility, Bloomington, Indiana 47405

We report recent measurements which are consistent with the co-existence of both fully equilibrated and non-equilibrium sources for IMF production in the reaction of 198.6 MeV ^3He ions with $^{\text{nat}}\text{Ag}$. The experiment was performed at the Indiana University Cyclotron Facility with a 50-100 nA ^3He beam incident upon a freshly-prepared self-supporting target of 1.99 mg/cm² $^{\text{nat}}\text{Ag}$. Blank runs indicated no IMF background due to any beam halo striking the target frame. Intermediate-mass-fragment charges were identified in a telescope consisting of a gas-ionization ΔE detector operated at 8 Torr of isobutane and a silicon E detector of thickness 170 μm . The high-energy tails of some Li - B spectra were affected by punch-through in the E detector. Corrections for target and ion-chamber window thicknesses were applied to the energy spectra.

The center-of-mass angular distributions observed in this experiment exhibit significant forward-peaking, with anisotropies decreasing from $\sigma(10^\circ)/\sigma(90^\circ) \approx 10$ for $Z = 5$ down to ≈ 4 for $Z = 11$ fragments. On the other hand, the differential cross sections beyond $\theta_{\text{cm}} \sim 90$ deg for all Z -values are essentially isotropic, indicative of equilibrium emission from a source with relatively low angular momentum. Figure 1 shows a rapidity plot for carbon fragments which is typical of the results for all IMF products. The invariant cross sections at large angles (> 80 degrees) fall on constant contour loci (semi-circles) expected for isotropic emission from a source moving with an average velocity $\beta \approx 0.0103$ ($\pm .0010$), nearly equal to that of the compound nucleus ($\beta_{\text{CN}} = 0.0104$). In contrast, the forward-angle data are skewed to much

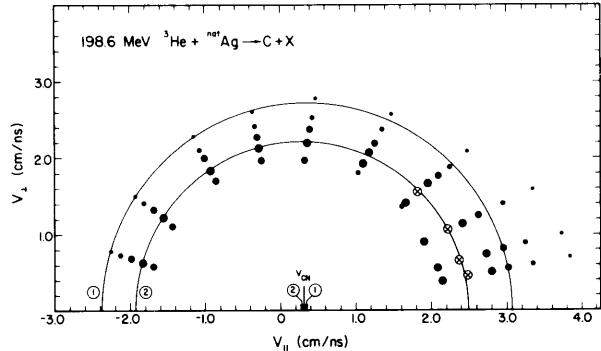


Figure 1. Plot of the invariant cross-section for carbon fragments in the $(v_{\parallel}, v_{\perp})$ plane. The diameter of the dots is proportional to the cross sections, with adjacent dots differing by a factor of ~ 2 ; the symbol \otimes indicates the position of the maxima in the forward angle spectra, which are higher in magnitude than at larger angles; the two semicircles are centered about v_{CN} , which corresponds to the compound nucleus velocity.

larger velocities, indicating emission from a faster moving source.

In Fig. 2 we show fragment energy spectra as a function of laboratory angle for $Z = 6$ fragments, characteristic of all the $Z \geq 4$ data. At forward angles one observes a Maxwell-Boltzmann-like energy distribution with a pronounced high-energy tail that systematically increases in slope as a function of increasing angle.¹⁻⁴ At larger angles the spectra evolve toward more Gaussian shapes, as is shown in Fig. 3, where spectra for $Z = 5-10$ fragments detected at an angle of 117 degrees are presented. The most probable center-of-mass kinetic energies associated with all backward-angle spectra ($\theta > 100$ deg) are consistent with two-body decay from a composite system. For low Z fragments these values correspond to tangent sphere acceleration with two-body kinematics, where the Coulomb radius $R_c = 1.225 (A_1^{1/3} + A_2^{1/3}) + 2.0$ fm. For $Z \geq 10$, they more closely approximate fission fragment kinetic energy systematics.

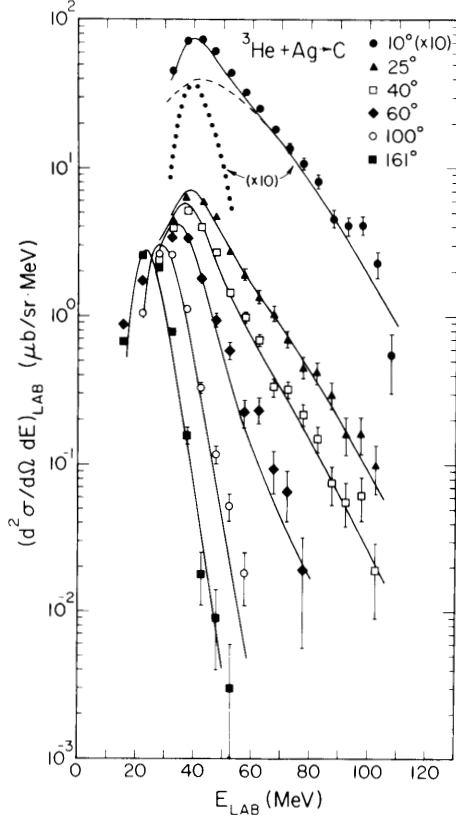


Figure 2. Energy spectra of carbon fragments as a function of angle. Data at 10 deg are multiplied by 10. Solid line is the fit of eq. (1); dashed line represents $\sigma_{NE}(E)$ and dotted line $\sigma_{EQ}(E)$. Data beyond 106 MeV are cut out due to particles punching through the detector.

On the basis of the angular distributions, rapidity analyses and kinetic energy spectra, we adopt a two-source model for the interpretation of these data. One component assumes statistical emission of IMFs from a fully equilibrated compound nucleus whereas the second is approximated by a fast-moving, thermal source.^{1,3,5} The data are fitted with a functional form:

$$\left(\frac{d^2\sigma}{d\Omega dE} \right)_Z = \sigma_{EQ} f_1(\beta_1, T_1, p_z, k_1) + \sigma_{NE} f_2(\beta_2, T_2, k_2) \quad (1)$$

where β_1 is the source velocity, T_1 is a temperature parameter, p_z is a Z-dependent amplification parameter⁶ and k_1 is the fractional Coulomb barrier. The total cross-sections for the equilibrium and non-equilibrium components for a fragment Z are given by σ_{EQ} and σ_{NE} ,

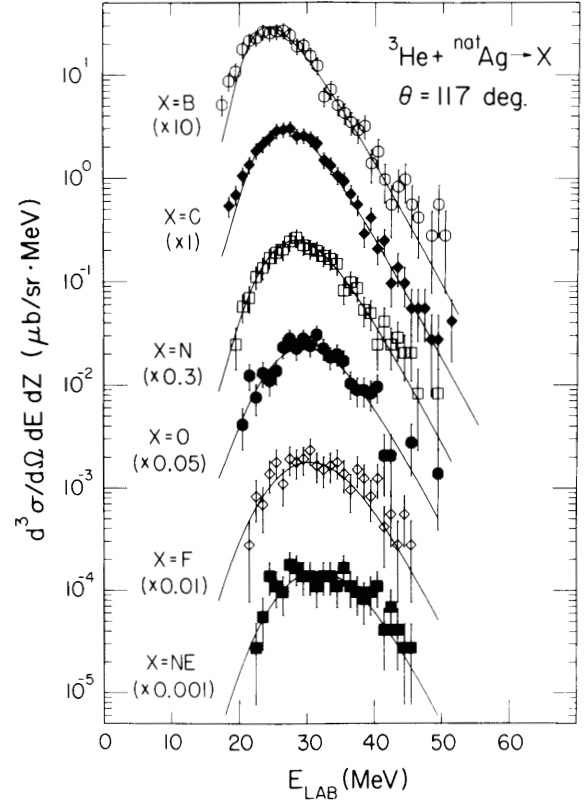


Figure 3. Laboratory energy spectra of IMF's with $5 < Z \leq 10$ at 117 degrees. Solid line represents the fit of eq. (1) to data.

respectively. The functions f_1 and f_2 contain appropriate kinematic transformations from the moving frame to the laboratory system and allow for recoil corrections.

The equilibrium component is described by the transition-state formalism of Moretto.⁶ Based on the rapidity plots, a source velocity $\beta_1 = \beta_{CN}$ is chosen. Correspondingly, we assume the temperature of the compound nucleus, $T_1 = T_{CN} = 3.7$ MeV, assuming $a = A/8$ MeV⁻¹. (A free parameter search yields β_1 and T_1 within 7% of these values.) The remaining parameters are then determined by the search routine. This parametrization alone provides a good fit to fragment energy spectra for $4 < Z < 12$ at $\theta_{LAB} > 100^\circ$ for light fragments and $\theta_{LAB} > 80^\circ$ for $Z > 8$. The results agree

well with the predicted [6] evolution in spectral shapes from Maxwellian for low-Z IMFs toward Gaussian for the heavier fragments as shown in Fig. 3.

Whereas the backward-angle data can be described well in terms of emission from a fully equilibrated compound nucleus, the forward-angle spectra appear to be increasingly dominated by more direct processes. This is shown in Fig. 2 for $Z = 6$ fragments at 10 degrees, where the equilibrium component calculated for this angle is shown by the dotted line. Consistent with previous analyses of IMF spectra^{1,3,5}, we have attempted to fit the non-equilibrium component (dashed line) with a Maxwell-Boltzmann source parametrization with surface emission, $f_2 \propto E'e^{-E'/T}$, where E' is the fragment kinetic energy in the moving frame.⁵ Good fits were obtained over the full angular range (Fig. 2) for $Z = 5$ to 10 fragments. The parameters of the non-equilibrium component were nearly Z -independent with $\beta_2 \approx 5\beta_{CN}$, $T_2 \approx 8$ MeV and $k_2 \approx 0.25$, if a gaussian Coulomb barrier distribution is assumed.⁴

The isotopic cross-sections associated with σ_{NE} exhibit a $Z^{-5.3}$ dependence. This is much stronger than the $Z^{-2.6}$ dependence derived from the total yields and

observed in high-energy studies.^{1,2} This analysis stresses the importance of removing the global equilibrium component of the IMF spectra prior to comparing data with purely non-equilibrium models. Because of the broad continuum of deposition energies which accompany reactions above $E/A \approx 30$ MeV, equilibrium emission provides an underlying background which modifies IMF spectra at intermediate energies. Hence, in order to understand the mechanisms of IMF emission, exclusive measurements must be performed which characterize the emitting source.

[†]Present address: Department of Physics, University of North Carolina, Chapel Hill, North Carolina 27514

- 1) A.M. Poskanzer et al., Phys. Rev. C 3, 882 (1971).
- 2) J.E. Finn et al., Phys. Rev. Lett. 49, 1321 (1982); R.W. Minich et al., Phys. Lett. 118B, 458 (1982).
- 3) R.E.L. Green and R.G. Korteling, Phys. Rev. C 22, 1594 (1980).
- 4) D.J. Fields et al., Phys. Rev. C 30, 1912, (1984); C.B. Chitwood et al., Phys. Lett. 131B, 289 (1983).
- 5) G.D. Westfall et al., Phys. Rev. C 17, 1368 (1978).
- 6) L.G. Moretto, Nucl. Phys. A247, 211 (1975).